

Supplementary Data

Disentangling social networks from spatiotemporal dynamics: the temporal structure of a dolphin society

M. Cantor*, L. L. Wedekin, P. R. Guimarães, F. G. Daura-Jorge, M. R. Rossi-Santos & P. C. Simões-Lopes

* Correspondence: M. Cantor, Laboratório de Mamíferos Aquáticos, Departamento de Ecologia e Zoologia, Universidade Federal de Santa Catarina, Caixa Postal 5102, CEP 88040-970, Trindade, Florianópolis, SC, Brazil.

E-mail address: m.cantor@ymail.com (M. Cantor).

Table of Contents

Supplementary Data S1. Modularity analysis details	02
Figure S1. Modularity under an increasing HWI cutoff scenario	03
Supplementary Data S2. Effect of observation threshold on network structure	04
Figure S2. Sighting frequency and network structure for three observation thresholds	05
Table S1. Overview of the null models	06
Table S2. Candidate exponential decay models for lagged association rates (LAR)	07
Table S3. Candidate exponential decay models for lagged identification rates (LIR)	08
Supplementary Data S3. HWI within and between sighting periods and network modules	09
Figure S3. Mean HWI within and between classes (modules, sighting periods)	10
Supplementary Data S4. Local network properties and the modular structure	11
Figure S4. Social network distance and centrality within and between sighting periods	13
Figure S5. LAR analysis within 32-month periods	14
References	15

Supplementary Data S1

Modularity Analysis Details

The modularity algorithm used here (Guimerà & Amaral 2005a, b) is based on a stochastic optimization process (Guimerà et al. 2004), and thus the results might vary for different runs. To explore the consistency of the modular topology of the Guiana dolphin social network, we ran the analysis 50 times (for a similar approach, see Donatti et al. 2011). We then calculated the similarity among the modules yielded in each run with the Sorensen index, which takes the double-presence of an individual in the modules as reference for resemblance. All of the runs divided the network into three modules when modularity was maximized at $M > 0.202$. Even though these values were slightly below the arbitrary 0.3 cutoff that hypothetically indicates good partitions by other algorithms (Newman 2004), all of them were significantly higher than expected by chance (using the null model NM2 described in the main text). Even though a few individuals were assigned to different modules across the runs, the resultant modules were highly similar (mean similarity \pm SD: Module 1 = 0.95 ± 0.05 ; Module 2 = 0.70 ± 0.18 ; Module 3 = 0.89 ± 0.08). Therefore, the observed network division was consistent.

To evaluate how consistent the modularity was when the weighted edges were taken into account, we simulated an increasing cutoff scenario using the association indices (HWI, which ranged from 0.1 to 1.0) to define an interaction (for a similar approach see de Silva et al. 2011). In each HWI cutoff, we (1) tested the modularity significance (see the null model NM2) and (2) quantified how similar the new filtered modules were to the unfiltered ones (using the Sorensen index as above). The modularity was relatively consistent under the increasing cutoff scenario. The majority of the HWI cutoffs yielded a higher modularity than that expected by chance. The modularity remained consistent until a cutoff of double the mean population association (HWI cutoff = 0.3; Fig. S1a), when there were low qualitative changes between the new modules and the unfiltered network modules (the similarity remained high, Fig. S1c). Moreover, the network broke into disconnected components only after the 0.3 HWI cutoff (Fig. S1b).

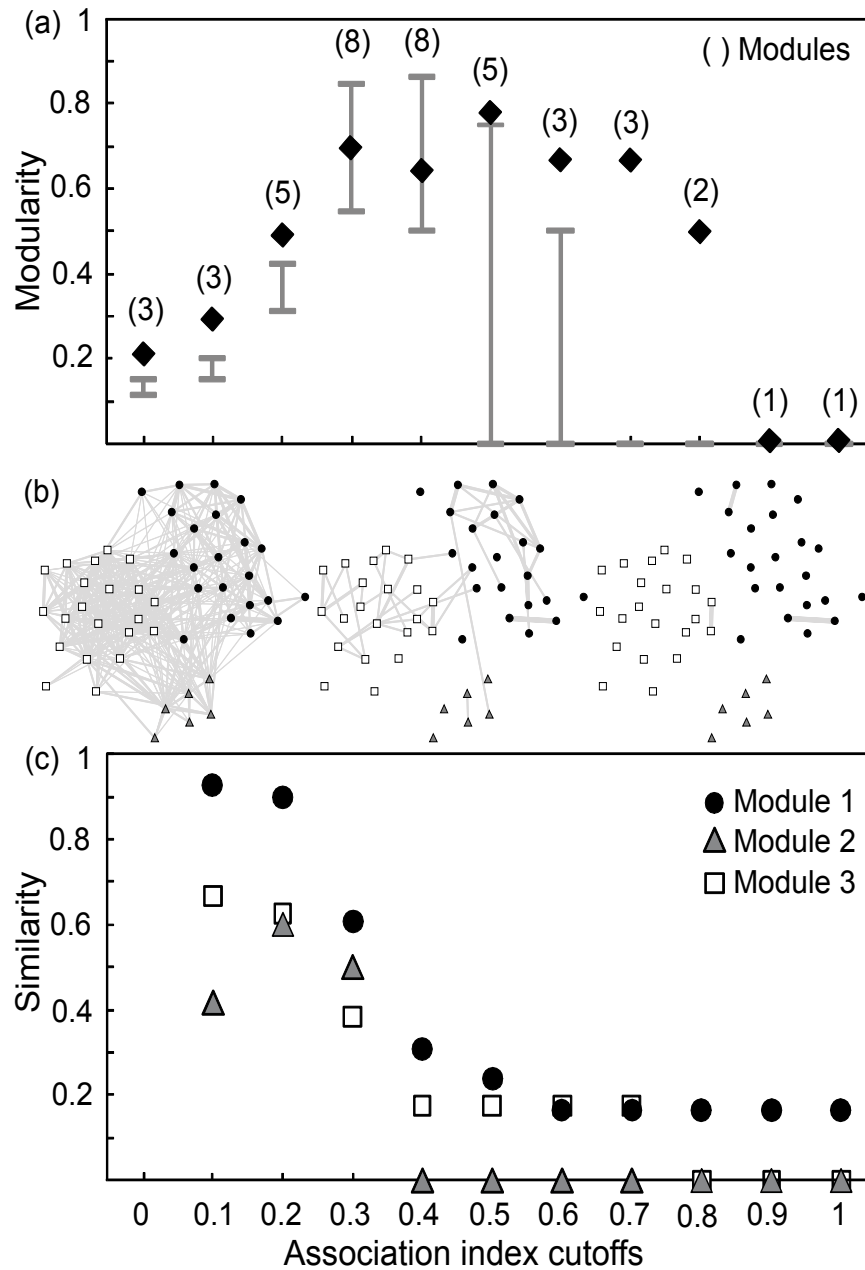


Figure S1. (a) Modularity of the social network of Guiana dolphins under an increasing association index cutoff scenario for defining a binary dyadic association. Whiskers represent the 95% confidence intervals generated using null model NM2. Parentheses indicate the number of modules in each cutoff. (b) Network breakdown due to HWI filtering: the first graph (left) represents the unfiltered network, the second graph represents a network filtered at 0.3 HWI, and the third graph represents a network filtered at 0.6 HWI or higher. After a 0.3 HWI cutoff, the network broke into disconnected components. (c) Higher similarities between the new filtered modules and the unfiltered modules were found until the 0.3 HWI cutoff.

Supplementary Data S2

Effect of Observation Threshold on Network Structure

To evaluate the network structure consistency due to the removal of infrequently observed individuals, we calculated the clustering coefficient ($C_{w,am}$) and modularity (M) under different observation thresholds (Fig. S2). When we excluded individuals that used the area sporadically, the social organization was restricted to the core of resident individuals ($N > 10$ resightings). In this case, the network would be highly clustered ($C_{w,am} = 0.928$, 95% CI = 0.900–0.917) and the modular structure would be dismantled ($M = 0$). However, by including transient dolphins ($N > 3$, $N > 5$ resightings) (see Cantor et al. 2012), another level of complexity emerged: a modular structure related to population turnover (see Figs 2, S2). Network metrics were consistent for the different thresholds that included transient individuals. Regardless of whether $N > 3$ or $N > 5$ was used, the clustering coefficient was moderate ($N > 3$: $C_{w,am} = 0.665$, 95% CI = 0.586–0.659; $N > 5$: $C_{w,am} = 0.757$, 95% CI = 0.705–0.732) and the network was significantly defined by three modules ($N > 3$: $M = 0.209$, 95% CI = 0.110–0.129; $N > 5$: $M = 0.142$, 95% CI = 0.038–0.0528; CIs were generated using null models, see Table S1). Since the properties of our studied network were consistent under $N > 3$ and $N > 5$ observation thresholds, we truncated the individuals resighted less than three times, adding the opportunity to explore the demographic effect and increasing our sample size by 30% (Fig. S2).

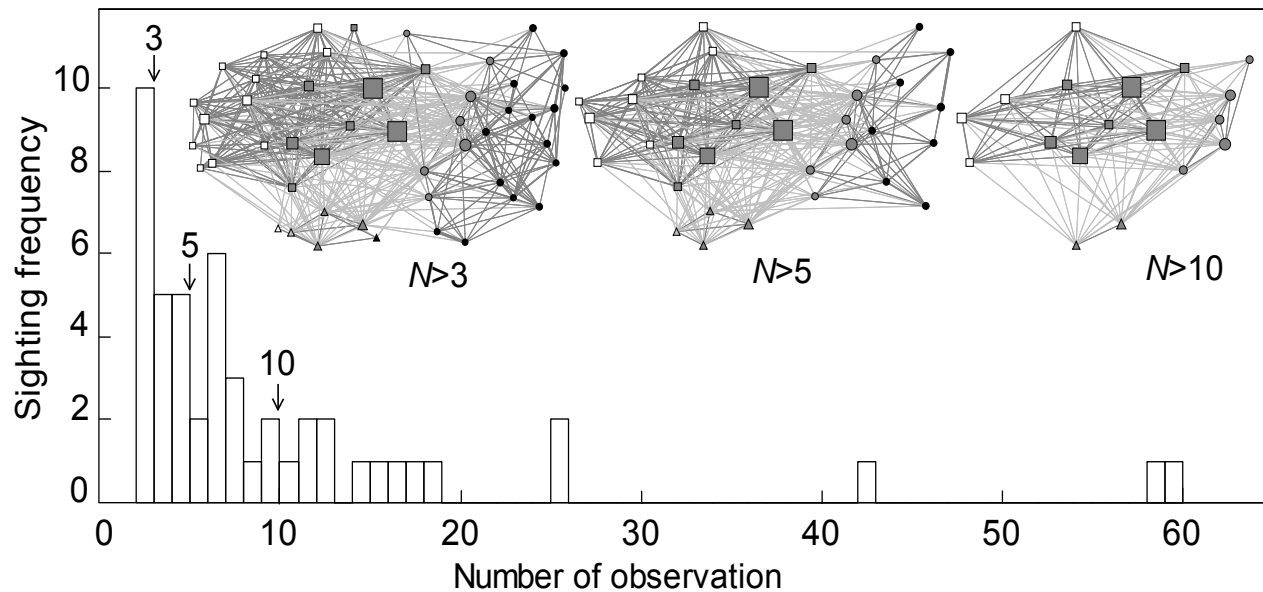


Figure S2. Histogram of sighting frequency (number of observations) of individual dolphins in the Caravelas River estuary and the subsequent social network structure for three observation thresholds ($N>3$, $N>5$, $N>10$ sightings). Social networks depict individuals (i.e. nodes whose sizes are proportional to the number of sightings) connected by the strength of associations (edges whose thicknesses are proportional to the association index). White and black nodes indicate transient dolphins sighted at the beginning and end of the study; grey nodes indicate resident dolphins sighted throughout the entire study. By including transient dolphins (either $N>3$ or $N>5$ sightings), another structure emerged comprising three modules related to population turnover (M1: square, M2: triangle, M3: circle) (see also Fig. 2 in main text).

Table S1

Overview of the three null models used to generate different benchmark distributions for hypothesis testing (see text)

Null model	What was randomized?		What was constrained?	
	Data structure	Biological interpretation	Data feature	Biological interpretation
NM1	Six binary matrices of individuals (rows) and integer periods of time (6, 8, 12, 16, 32 and 48 months)	Identified dolphins among different periods of the entire study period	Row sums	Number of times individuals were sighted during the entire study
NM2	Binary matrix of individuals (columns) and groups (rows)	Identified dolphins into observed groups	Row and column sums	Group size and individual sighting frequency
NM3	Binary matrix of individuals (rows) and network modules (columns)	Identified dolphins into network partitions defined by the modularity analysis	Column sums	Module size

Table S2

Candidate exponential decay models ranked by lowest quasi-Akaike Information Criterion (QAICc) for lagged association rates (LAR) of Guiana dolphins between 2002 and 2010

LAR models	Biological interpretation	QAICc	Δ QAICc
$g(d) = P_{\text{cas}} \times e^{-d/\tau_{\text{cas}}}$	Rapid dissociation + casual acquaintances	11 482.1	0
$g(d) = P_{\text{cas}} \times e^{-d/\tau_{\text{cas}}} + P_{\text{perm}} \times e^{-d/\tau_{\text{perm}}}$	Rapid dissociation + two levels of casual acquaintances	11 484.6	2.5
$g(d) = P_{\text{cas}} \times e^{-d/\tau_{\text{cas}}} + (1 - P_{\text{cas}}) \times e^{-d/\tau_{\text{perm}}}$	Two levels of casual acquaintances	11 530.3	48.2
$g(d) = P_{\text{cc}} + P_{\text{cas}} \times e^{-d/\tau_{\text{cas}}}$	Rapid dissociation + constant Companionship + casual acquaintances	11 657.5	175.4
$g(d) = P_{\text{cc}} + (1 - P_{\text{cas}}) \times e^{-d/\tau_{\text{cas}}}$	Constant companionship + casual acquaintances	11 724.9	242.8
$g(d) = P_{\text{cc}}$	Rapid dissociation + constant companionship	11 733.3	251.2
$g(d) = e^{-d/\tau_{\text{cas}}}$	Casual acquaintances	18 919.7	7437.6

Association rates between individuals (g), given as a function of time lag (d), was related to the proportion of constant companions (P_{cc}) and the proportion of casual acquaintances (P_{cas}) that lasted for a particular length of time (τ_{cas}), and to the proportion of casual associations (P_{perm}) that lasted for a longer period (τ_{perm}) (see Whitehead 1995).

Table S3

Candidate exponential decay models ranked by lowest quasi-Akaike Information Criterion (QAICc) for lagged identification rates (LIR) of Guiana dolphins between 2002 and 2010

LIR models	Biological interpretation	QAICc	Δ QAICc
$R(d) = N^{-1} \times e^{-\lambda \times d}$	Emigration/mortality	40 430.7	0
$R(d) = N^{-1} \times e^{-d/a}$	Emigration/mortality	40 430.7	0
$R(d) = \frac{N^{-1} \times ((b^{-1}) + (a^{-1}) \times e^{-(b^{-1} + a^{-1}) \times d})}{(b^{-1} + a^{-1})}$	Emigration + reimmigration	40 432.7	2.0
$R(d) = \frac{(e^{-(\delta \times d/N)}) \times ((b^{-1}) + (a^{-1}) \times e^{-(b^{-1} + a^{-1}) \times d})}{(b^{-1} + a^{-1})}$	Emigration/mortality + reimmigration	40 434.3	3.7
$R(d) = b \times e^{(-N \times d)} + \delta \times e^{(-a \times d)}$	Emigration/mortality + reimmigration	40 434.6	3.9
$R(d) = a_2 + a_3 \times e^{(-\lambda \times d)}$	Emigration + reimmigration	40 838.4	407.7
$R(d) = 1/N$	Closed population	40 846.7	416.0

Identification rates of individuals (R), given as a function of time lag (d), was related to the following parameters: population size (N), mean residence time in the study area (a), mean time out of the study area (b), emigration rate (λ) and mortality rate (δ); other parameters (a_2 , a_3) can be reparameterized as the proportion of the population in the study area at any time ($a_2/(a_2 + a_3)$) and to estimate immigration rate (μ), where $a_2 = \lambda/(N \times (\lambda + \mu))$ and $a_3 = \mu/(N \times (\lambda + \mu))$; see Whitehead (2001).

Supplementary Data S3

HWI within and among Sighting Periods and Network Modules

To further test the relationship between the emergence of modules in the social network of Guiana dolphins and the temporal effect, we compared the average association indices within and among modules or sighting periods (see main text). We expected individuals sighted in the same period (or present in the same module) to show association indices significantly higher than those of individuals from different periods (or modules). The observed associations were calculated using the half-weight index (HWI), while random HWIs were generated using the null model NM3 described in the main text. The comparison among and within modules or periods was carried out using a Mantel test on the null hypothesis that the association among and within them would be similar (Schnell et al. 1985).

The association levels were higher than the random values among individuals classified according to the sighting periods (Mantel test: $t_{\infty} = 7.555$, $r = 0.248$, $P = 1$). The mean HWIs among individuals sighted only at the beginning, only at the end or throughout the entire study period were higher than those expected by chance. In contrast, the HWIs among individuals of different sighting periods were lower than those expected by chance (Fig. S3). The same pattern was found for the association level of individuals classified using the network modules: mean HWI values were higher than expected within the modules, and lower among them (Mantel test: $t_{\infty} = 13.3278$, $r = 0.410$, $P = 1$; Fig. S3). These results strengthen the relationship between the differences in the presence of individuals in the population throughout the study and the emergence of modules.

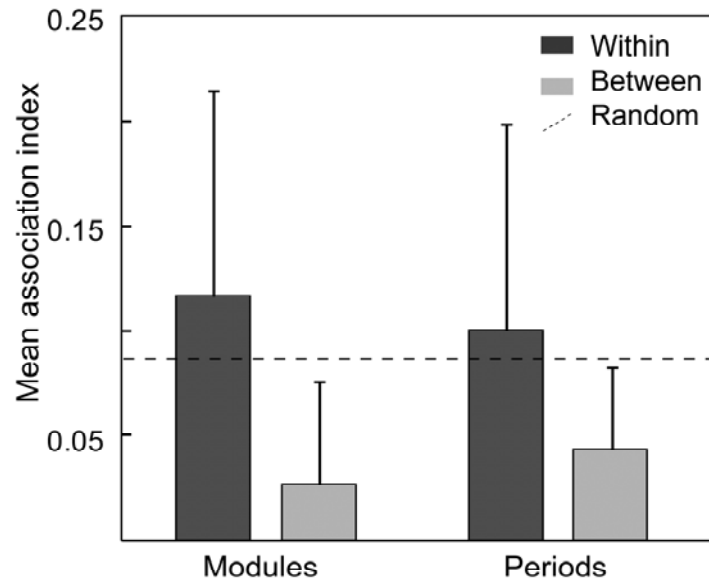


Figure S3. Mean association (HWI) of Guiana dolphins within and among classes: the three modules of the social network (see Fig. 2a of the main text) and the three sighting periods (at the beginning or end of the study period, or throughout the study period; see main text). Random values represent the mean HWI generated using null model NM3. Whiskers represent the 95% CI.

Supplementary Data S4

Local Network Properties and the Modular Structure

We further tested whether the demographic effect (turnover of individuals in the population) affected the network structure by analysing the relationship between local network measures and emergence of modules. We compared small path length (SPL) and a centrality measure among the individuals of different sighting periods (Beginning, End and All; see main text) and compared the results with the null expectation generated using null model NM3 described in the main text.

The SPL is the minimum distance between two individuals in the network. We expected a lower average SPL among individuals from the same sighting period but a higher mean SPL among individuals of different periods. In weighted social networks, the SPL is better described by the lowest sum of the inverse of an edge's weight (see Opsahl et al. 2010); thus, we used the inverse of the association index ($1/HWI$) as a measure of the distance between two individuals (the proportion of time that they were disassociated). We exponentiated the edge weights to $\alpha = 2$ to focus on the stronger interactions (see Opsahl et al. 2010).

Centrality measures allow for the identification of different positions in the social network, such as the positions of central and peripheral individuals (see Krause et al. 2010). Our expectation was that individuals sighted within the same sighting periods would occupy the same social positions in the network. For each node, we calculated the weighted counterparts of the three classic centrality measures (closeness, betweenness, degree; see definitions in: Freeman 1978; Opsahl et al. 2010). To ensure that both the edge weights and the number of intermediary nodes affected the centrality, we used four values for the tuning parameter proposed by Opsahl et al. (2010): $\alpha = 0$, $\alpha = 0.5$, $\alpha = 1$, $\alpha = 2$. When $\alpha = 0$, the metrics are binary, while for $\alpha = 1$, the metrics are weighted. Values of $\alpha \in [0,1]$ prioritize the number of intermediary nodes at the expense of the strength of interactions. By contrast, when $\alpha > 1$, additional intermediary nodes are less important than the strength of interactions. The analyses

were programmed in the R environment using the tnet package (R Development Core Team 2011; also see Opsahl 2009). To select the most influential measure, we applied a principal components analysis (PCA; see Estrada 2007). The PCA analysis identified closeness, at $\alpha = 0.5$, as the most representative of the 12 centrality variables (eigenvector coordinates: Factor 1 = -0.951, Factor 2 = 0.081; PC 1 and PC 2 accounted for 80.7% of the variation).

Dolphins within a sighting period were more cohesively connected than dolphins sighted between periods (Fig. S4a, b), reflecting their segregation into network modules. Average SPL within individuals sighted at the beginning and end of the study were lower than expected (Fig. S4a), while the length between them was higher than expected (Fig. S4b). Also, as expected, individuals sighted throughout the study were less cohesive (nonsignificant differences in SPL within and between periods: Fig. S4a, b) and were equally distributed across the three modules. The Guiana dolphins' centrality varied between the classes of sighting period, suggesting that individuals occupied different positions in the network that were coupled with the modular topology. Dolphins that were present in the population only at the beginning or at the end of the study occupied peripheral positions in the network (less central than expected: Fig. S4c), reinforcing their segregation into distinct modules. In contrast, dolphins sighted throughout the study were more central (Fig. S4c). As residents, these individuals were frequent in the area and associated with transient individuals. Therefore, the resident central individuals were equally distributed across the three modules. This arrangement identified them as the core of the population.

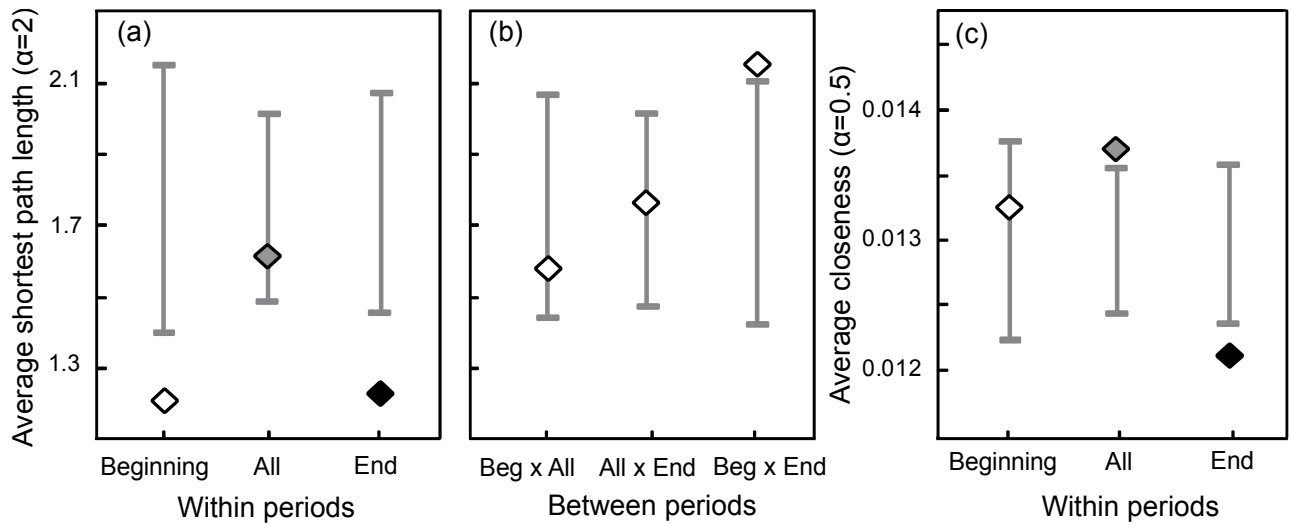


Figure S4. Social network distance and centrality of Guiana dolphins classified by the period of the study during which they were sighted (Beginning, End, All; see main text for details). Average weighted shortest path length (a) within and (b) between sighting periods. (c) Average weighted closeness within periods. Whiskers represent the 95% CI generated using null model NM3 (see main text).

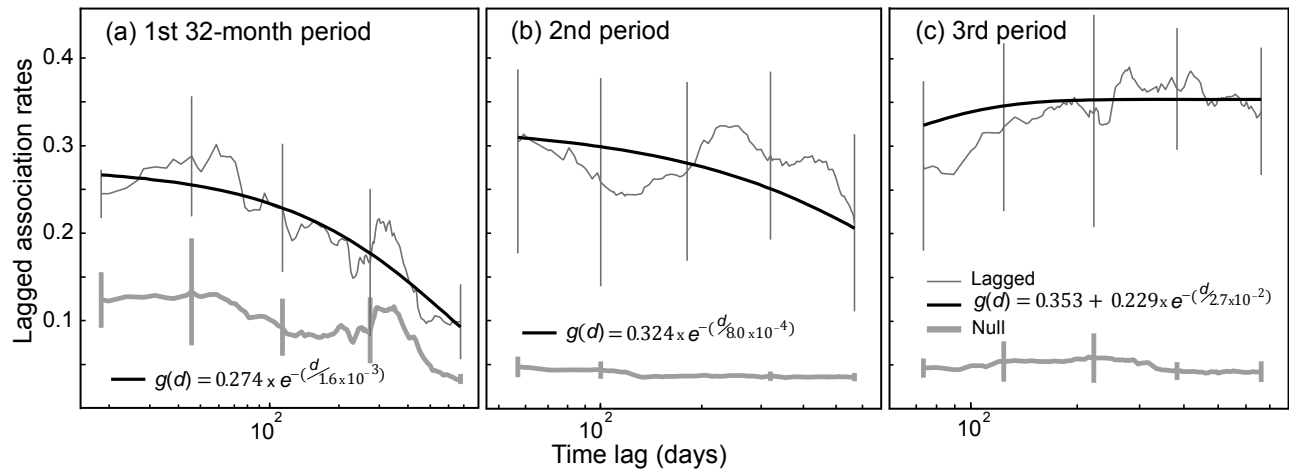


Figure S5. Lagged association rate (LAR) analyses for Guiana dolphins sighted within the population turnover scale. The seven models described in Table S1 were fitted to the data set into three 32-month periods. LAR values within the (a) first and (b) second periods were best described using a model composed of rapid dissociations and casual acquaintances (the same first model in Table S2). The best fitted model for the third period was also composed of rapid dissociations and casual acquaintances in addition to constant companionships (see fourth model, Table S2). In all of the periods, no other model received significant support ($\Delta\text{QAICc} > 2$), and the LAR values were nonrandom, as evidenced by the fact that the LAR values remained higher than the null association rates (see Whitehead 1995). These outcomes demonstrated that, after excluding the demographic effect, the fluid grouping pattern tended to be the same as the grouping pattern observed for the entire study (see Fig. 4a, Table S2). Note, however, that models describe the LAR and not social organization per se; thus, the parameter labels denote only the temporal patterning of associations.

References

- Cantor, M., Wedekin, L. L., Daura-Jorge, F. G., Rossi-Santos, M. R. & Simões-Lopes, P. C.** 2012. Assessing population parameters and trends of Guiana dolphins (*Sotalia guianensis*): an eight-year mark–recapture study. *Marine Mammal Science*, **28**, 63–83.
- Donatti, C. I., Guimarães, P. R., Jr, Galetti, M., Pizo, M. A., Marquitti, F. M. D. & Dirzo, R.** 2011. Analysis of a hyper-diverse seed dispersal network: modularity and underlying mechanisms. *Ecology Letters*, **14**, 773–781.
- Estrada, E.** 2007. Characterization of topological keystone species local, global and ‘meso-scale’ centralities in food webs. *Ecological Complexity*, **4**, 48–57.
- Freeman, L. C.** 1978. Centrality in social networks: conceptual clarification. *Social Networks*, **1**, 215–239.
- Guimerá, R. & Amaral, L. A. N.** 2005a. Cartography of complex networks: modules and universal roles. *Journal of Statistical Mechanics: Theory and Experiment*, **2005**, P02001, doi:10.1088/1742-5468/2005/02/P02001.
- Guimerá, R. & Amaral, L. A. N.** 2005b. Functional cartography of complex metabolic networks. *Nature*, **433**, 895–900.
- Guimerá, R., Sales-Pardo, M. & Amaral, L. A. N.** 2004. Modularity from fluctuations in random graphs and complex networks. *Physical Review E*, **70**, 025101.
- Krause, J., James, R. & Croft, D. P.** 2010. Personality in the context of social networks. *Philosophical Transactions of the Royal Society B*, **365**, 4099–4106.
- Newman, M. E. J.** 2004. Analysis of weighted networks. *Physical Review E*, **70**, 056131.
- Opsahl, T.** 2009. Structure and evolution of weighted networks. Ph.D. thesis, University of London.
- Opsahl, T., Agneessens, F. & Skvoretz, J.** 2010. Node centrality in weighted networks: generalizing degree and shortest paths. *Social Networks*, **32**, 245–251.
- R Development Core Team** 2011. *R: a Language and Environment for Statistical Computing*. Vienna, Austria: R Foundation for Statistical Computing. <http://www.R-project.org>.

- Schnell, G. D., Watt, D. J. & Douglas, M. E.** 1985. Statistical comparison of proximity matrices: applications in animal behaviour. *Animal Behaviour*, **33**, 239–253.
- de Silva, S., Ranjeewa, A. D. G. & Kryazhimskiy, S.** 2011. The dynamics of social networks among female Asian elephants. *BMC Ecology*, **11**, 17.
- Whitehead, H.** 1995. Investigating structure and temporal scale in social organizations using identified individuals. *Behavioral Ecology*, **6**, 199–208.
- Whitehead, H.** 2001. Analysis of animal movements using opportunistic individual identifications: application to sperm whales. *Ecology*, **82**, 1427–1432.